Nicastrin regulates breast cancer stem cell properties and tumor growth in vitro and in vivo

Ylenia Lombardo[a,1], Aleksandra Filipović[a,1], Gemma Molyneux[a], Manikandan Periyasamy[a], Georgios Giamas[a], Yunhui Hu[a], Pritesh S. Trivedi[b], Jayson Wang[b], Ernesto Yagüe[a], Loren Michel[c], and R. Charles Coombes[a]

[a]Division of Surgery and Cancer, Department of Oncology, Imperial College London, Hammersmith Hospital Campus, W12 0NN, London, United Kingdom; [b]Department of Histopathology, Imperial College Healthcare NHS Trust, Hammersmith Hospital Campus, W12 0NN, London, United Kingdom; and [c]Division of Oncology, Department of Internal Medicine, Washington University School of Medicine, St. Louis, MO 63110

Edited* by Jan-Åke Gustafsson, Karolinska Institutet, Huddinge, Sweden, and approved August 24, 2012 (received for review April 17, 2012)

Nicastrin (NCT) is a crucial component of the γ-secretase (GS) enzyme, which prompted investigations into its biological role in cancer. We have previously shown that nicastrin is overexpressed in breast cancer (BC), conferring worse overall survival in invasive, ERα negative patients. Here, we used 2D and 3D Matrigel, anchorage-independent growth conditions and a breast cancer xenograft mouse model to assess the impact of nicastrin on breast cancer stem cell (BCSC) propagation and invasion in vitro and tumor growth in vivo. Stable knockdown of nicastrin in HCC1806 breast cancer cells reduced cell invasion by 51.4 ± 1.7%, accompanied by a morphological change to a rounded cell phenotype and down-regulation of vimentin, Snail, Twist, MMP2, and MMP9. We observed a reduction of the pool of $CD44^+/CD24^-$ and ALDH1 high breast cancer stem cells by threefold and twofold, respectively, and a reduction by 2.6-fold of the mammospheres formation. Nicastrin overexpression in nontransformed MCF10A cells caused an induction of epithelial to mesenchymal regulators, as well as a fivefold increased ALDH1 activity, a threefold enrichment for $CD44^+/CD24^-$ stem cells, and a 3.2-fold enhanced mammosphere-forming capacity. Using the γ-sescretase inhibiton, Notch1/4 siRNA, and Akt inhibition, we show that nicastrin regulates breast cancer stem cells partly through Notch1 and the Akt pathway. Exploiting serial dilution transplantation of the HCC1806 cells expressing nicastrin and HCC1806 stably depleted of nicastrin, in vivo, we demonstrate that nicastrin inhibition may be relevant for the reduced tumorigenicity of breast cancer cells. These data could serve as a benchmark for development of nicastrin-targeted therapies in breast cancer.

metastasis | mammary tumor

Emerging data suggest that tumor recurrence and poor clinical outcome of cancer patients may be due to the fact that a small subset of stem-like cells, called cancer stem cells (CSCs) (1), identified on the basis of a combination of $CD44^+/CD24^-$, and/or aldehyde dehydrogenase 1 (ALDH1) activity (2, 3), evade effects of systemic therapies. Alterations in critical signaling pathways such as Notch, Hedgehog, and Wnt allow stem cells to undergo uncontrolled proliferation and form tumors (4, 5).

Breast CSCs (BCSCs) are enriched for cells that can undergo epithelial–mesenchymal cell transition (EMT), which plays a role in metastases (6, 7). Moreover, BCSCs possess an "invasiveness" gene signature that correlates with poor overall survival in cancer patients (1), making it necessary to characterize CSC markers and signaling pathways that regulate the mammary stem cell population (8, 9). γ-Secretase (GS) is multiprotein enzyme complex, composed of presenilin 1 (PS1), nicastrin (NCT), anterior pharynx-defective phenotype 1 (APH-1), and the PS enhancer 2 (PEN-2) (10). It is responsible for the intramembranous cleavage and activation of various type-I membrane proteins such as Notch, CD44, HER4, etc. (11). Aberrant activation of these substrates has been implicated in tumorigenesis, metastasis, and development of resistance to existing treatment regimens in oncology (12–14).

γ-Secretase inhibitors (GSIs) (DAPT and MRK-003), which prevent Notch cleavage, genetic silencing of Notch1 and Notch4, as well as blocking Notch1 ligand activation using a monoclonal antibody (14–17), are all able to reduce mammosphere formation in vitro and number of tumor initiating cells in vivo, supporting the notion that targeting Notch signaling may facilitate durable tumor regression (15, 18). It has become apparent from phase I and II clinical trials using GSIs, that these compounds may have a dose-limiting toxicity profile, primarily concerning gastrointestinal goblet cell hyperplasia (19–21). In breast cancer (BC) cells, single agent GSI is not potent in inhibiting cell proliferation in vitro and in vivo. Only rare cell lines and patient tumors with a Notch fusion gene, which results in constitutively active Notch1, are susceptible to single agent GSI growth inhibition (22). This may represent a hindrance in the clinic, encouraging the efforts to explore alternative/additional modalities of targeting Notch/GS (23).

Recognition of NCT relevance for the synthesis and stability of the other GS components, as well as for GS-substrate recognition (24), has prompted investigations into its biological role in cancer. We have shown that NCT is overexpressed in 47.5% of BC patients, where its abundance confers worse overall survival in the ERα negative patients (25). Supporting the biological relevance of NCT in malignant disease, it has been demonstrated that NCT stable knockdown (shRNA) enhances antitumor effects of EGFR inhibitors by Notch and Akt inhibition (26), and that NCT is increased in response to chemotherapy in colon cancer (27). For this reason, we and others are considering targeting NCT using antagonistic monoclonal antibodies to intercept GS activity and NCT-driven signaling in cancer cells (25, 28).

Here, we have used a stable genetic silencing (shRNA) and overexpression approach to address the effects of NCT expression modulation on BCSCs and invasive properties. We demonstrate that stable knockdown of NCT in HCC1806 BC cells and stable overexpression in nontransformed MCF10A cells regulate GS/Notch and Akt activity, affect the proportion of BCSCs as defined by the $CD44^+/CD24^-$ and $ALDH1^+$ phenotype, and their invasive capacity through impingement on the EMT cellular regulators. Moreover, exploiting serial dilution transplantation in vivo, we confirm the importance of NCT depletion for the tumorogenicity of BC cells.

Results

Nicastrin Expression Affects Morphology, Growth, and Invasive Behavior of Breast Cells. To investigate the role of NCT in breast cells, we used stable NCT-knockdown HCC1806 BC cells (HCC1806-ShNCT) and stable NCT-overexpressing MCF10A epithelial mammary cells (MCF10ANCT). Nicastrin depletion and overexpression were confirmed in the relevant cell lines (Fig. S1*A*). We observed a significant morphological alteration after NCT depletion in HCC1806 cells,

Author contributions: Y.L. and A.F. designed research; E.Y., L.M., and R.C.C. designed experiments; Y.L. and A.F. performed research; G.M. performed RT-PCR; M.P. performed animal work; Y.H. performed soft agar assay; P.S.T. performed IHC; J.W. performed IHC interpretation; G.G. provided assistance with experiments, reagents, and animals; and Y.L., A.F., E.Y., L.M., and R.C.C. wrote the paper.

The authors declare no conflict of interest.

*This Direct Submission article had a prearranged editor.

[1]To whom correspondence may be addressed. E-mail: a.filipovic@imperial.ac.uk or y.lombardo@imperial.ac.uk.

This article contains supporting information online at www.pnas.org/lookup/suppl/doi:10.1073/pnas.1206268109/-/DCSupplemental.

where the spindle shape and the scattered distribution of control cells (HCC2806-ShLuc) changed to a rounded phenotype and compact cell clusters in HCC1806-ShNCT (Fig. 1*A*). Conversely, NCT-overexpressing cells demonstrated a transformation from cobblestone-like epithelial cells to a more elongated fibroblast-like morphology with cellular scattering, compared with control MCF10A cells (Fig. 1*A*). Proliferation rate of HCC1806-ShNCT cells was reduced by 47 ± 4.1% ($P < 0.01$) over the period of 6 d compared with HCC1806-ShLuc (Fig. 1*B*), similar to the effects of transient NCT knockdown by siRNA in MDAMB231 cells (Fig. S1*B*). Overexpression of NCT, however, did not affect the proliferation of MCF10A cells grown on 2D monolayers (Fig. S1*C*). We therefore used the more physiologically relevant 3D Matrigel-overlay model, allowing for the integration of crucial extracellular matrix signaling. In the 3D context, HCC1806-ShLuc cells formed grape-like complex acini structures, characterized by the absence of functional cell–cell adhesions and increased migratory behavior (29). Conversely, HCC1806-ShNCT cells yielded significantly smaller acini with the shape more closely resembling that of nonmalignant cells (Fig. 1*A*), suggesting that cells lacking NCT expression may have undergone a reversal of the EMT. Conversely, NCT overexpression in nontumorigenic MCF10A cells induced more rapidly proliferating acini-like structures in 3D Matrigel compared with the growth-arrested acini formed by MCF10A-Ctrl cells (Fig. 1*A*). Furthermore, activated Notch1 (N1ICD at ∼110 kDa) and Notch4 (N4ICD at ∼75 kDa, but note no change in ∼60 kDa and ∼40 kDa bands) were reduced in HCC1806-ShNCT cells and induced in MCF10ANCT cells, whereas Notch2 and Notch3 intracellular domain (ICD) remained unchanged (Fig. 1*C* and Fig. S1 *Fa* and *Fb*). Finally, we demonstrated that the expression levels of PEN-2, Aph-1, PS1 full length, as well as processed PS1–C-terminal fragment are reduced upon NCT depletion and increased upon NCT overexpression (Fig. 1*C* and Fig. S1*G*), whereas PS1 mRNA is modulated in the opposite manner (Fig. S1*H*). Given that PS1 protein levels are coordinately regulated in response to NCT expression modulation, this appears to initiate a feedback loop affecting PS1 transcription in the opposite manner. The exact mechanism behind this remains to be elucidated. Taken together, this confirms the role of NCT in regulating protein levels of the GS complex and activation of Notch1 and -4. Importantly, higher levels of pAkt were observed in NCT expressing cells, indicating a potential regulation of the PI3K/Akt pathway by NCT (Fig. 1*C*).

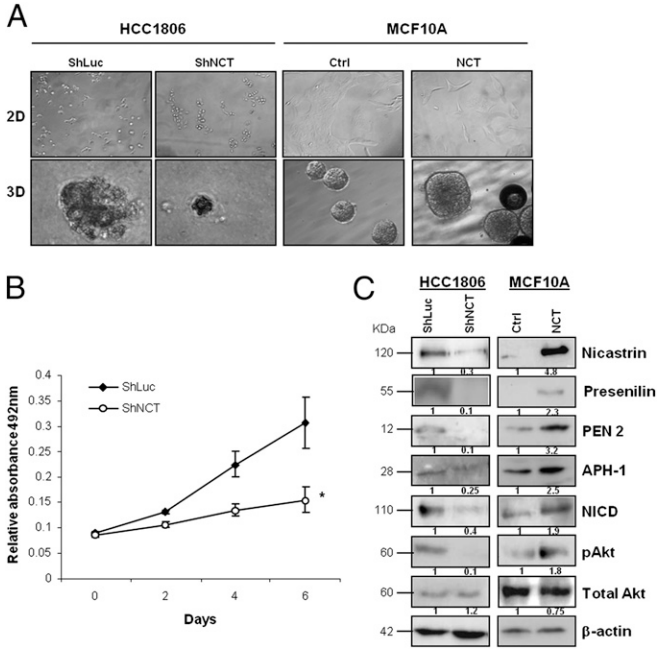

Fig. 1. Nicastrin expression affects morphological features and proliferation rate of breast cells. (*A*) Phase contrast microscopy of HCC1806-ShLuc, HCC1806-ShNCT, MCF10A-Ctrl, and MCF10ANCT cells cultured in 2D (*Upper*) and 3D Matrigel-overlay chambers (*Lower*); magnification 10×. Error bars are SEM of two independent experiments, each in quadruplicate, $*P = 0.017$. (*B*) Western blot confirming NCT knockdown in MDAMB231 cells; proliferation assay in MDAMB231 treated with 40 nmol of the *Control* siRNA, *NCT* siRNA, and the positive control *Death* siRNA. $*P = 0.005$. Error bars represent SEM of two separate experiments, each done in triplicate. (*C*) Western blotting analysis of HCC1806-ShLuc, HCC1806-ShNCT, MCF10A-Ctrl, and MCF10ANCT whole cell lysates with indicated antibodies. β-Actin was used as a loading control.

We next investigated the impact of NCT expression in the EMT markers and invasive capacity of breast cells. NCT depletion in HCC1806 significantly reduced cell invasion by 51.4 ± 1.7% (Fig. 2*A*, $P = 0.001$). This was accompanied by an inhibition of EMT regulators such as *vimentin*, *Snail*, *SIP1*, *MMP2*, and *MMP9* (Fig. 2*B*, $*P < 0.05$, $**P < 0.01$, $***P < 0.001$). These observations were confirmed in a panel of other BC cell lines (MDAMB231, MDAMB468, BT474, and SKBR3) upon transient NCT silencing (Fig. S2*A*). NCT overexpression in MCF10A cells increased levels of *vimentin*, *MMP2*, *MMP9*, *Twist1*, *Snail1*, and *SIP1*, demonstrating that, in a nontransformed breast epithelial cell line, high expression of NCT potently induces an EMT-related gene signature (Fig. 2*C*).

Nicastrin Expression Affects Expansion of the Breast Cancer Stem Cell Population. Because it has been shown that undergoing EMT can enrich for stem cells in BC, we tested the effect of NCT on the stem cell content, their mammosphere formation ability, and invasive features. Flow cytometry analysis of MCF10ANCT cells demonstrated a threefold increase in the $CD44^+/CD24^-$ population, compared with MCF10A-Ctrl cells (Fig. 3*A*) and a fivefold increase in the $ALDH1^{high}$ population within MCF10ANCT cells (Fig. 3*B* and Fig. S2*B*).

Consistent with this, the mammosphere formation assays showed a 3.2-fold increase in sphere-forming efficacy (SFE) of MCF10ANCT cells compared with control (Fig. 3 *C* and *D*). Conversely, suppression of endogenous NCT in HCC1806 cells led to a reduction of BCSCs defined by $CD44^+/CD24^-$ and $ALDH1^{high}$ phenotype by threefold and twofold, respectively, and coordinately inhibited the SFE by 2.6-fold (Figs. 2*A* and 3 *A*–*C*). Moreover, primary mammospheres from both HCC1806 and MCF10A cells were digested into single cells and assayed for their ability to form secondary mammospheres. NCT depletion and overexpression, respectively, maintained inhibition and even further enhanced SFE in the second passage (Fig. 3*C*). We further confirmed that in a panel of other BC cell lines (MCF7, MDAMB468, BT474, and SKBR3), transient NCT silencing was sufficient to decrease both the $CD44^+/CD24^-$ and the $ALDH1^{high}$ populations (Fig. S3 *A* and *B*).

We next checked whether NCT inhibition modulated transcription of the proinvasive genes in the putative stem cells in the HCC1806-ShLuc and HCC1806-ShNCT cell lines. We separated the "stem cells" ($CD44^+/CD24^-$ cells) from "nonstem cells" ($CD44^+/CD24^-$-depleted cells) in HCC1806-ShLuc and HCC1806-ShNCT cell lines by FACS sorting. Down-regulation of NCT mRNA levels was confirmed in respective HCC1806-ShNCT populations (Fig. S3*C*). The invasion assay demonstrated that the $CD44^+/CD24^-$ stem cell population within HCC1806-ShLuc cells is characterized by the highest invasive ability, which was threefold greater than that of the HCC1806-ShNCT stem cell counterpart. Depletion of NCT was sufficient to reduce cell invasion in both nonstem cells and in the stem cell population (Fig. 3*E*). Accordingly, vimentin was markedly overexpressed (8.5-fold) in the stem cell pool of the HCC1806-ShLuc cells, compared with the nonstem cells (Fig. 3*F*). Strikingly, NCT depletion was able to prevent an increase of vimentin mRNA in the stem cell pool of the HCC1806-ShNCT cell line, maintaining the levels comparable to those in the HCC1806ShNCT nonstem cells. The same trend was observed for *SIP1*, *Twist*, and *Snail1* (Fig. 3*F*). To ascertain that the observed effects on the proinvasive genes in HCC1806 ShNCT

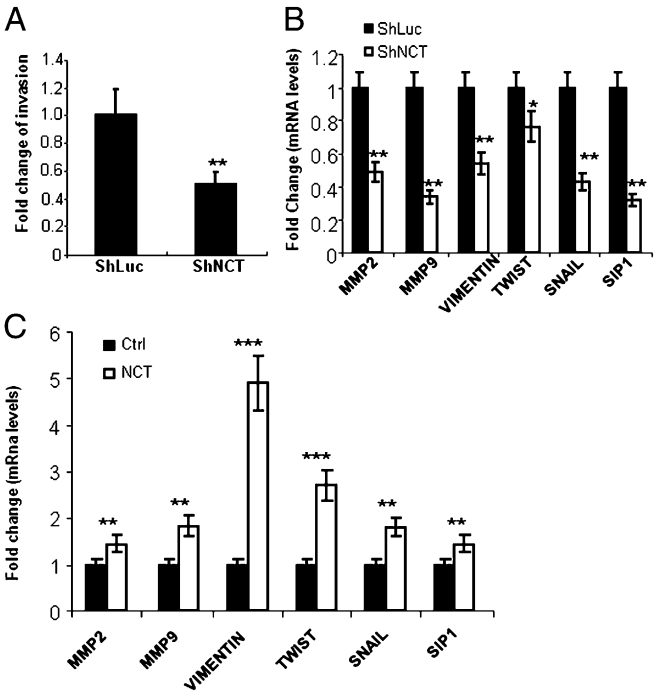

Fig. 2. Invasive behavior of breast cells and EMT genes is regulated by nicastrin. (*A*) Transwell invasion assay of HCC1806-ShLuc, HCC1806-ShNCT cells. Bars represent mean number of invaded cells ± SEM from three separate experiments, each in triplicate. $*P = 0.001$. (*B*) RT-qRT-PCR showing fold change of quantitative mRNA levels of *MMP2*, *MMP9*, *Vimentin*, *Twist*, *Snail*, and *SIP1* genes in HCC1806-ShNCT versus HCC1806-ShLuc cells. (*C*) RT-qPCR showing fold change of quantitative mRNA levels of *MMP2*, *MMP9*, *Vimentin*, *Twist*, *Snail*, and *SIP1* genes in MCF10ANCT versus MCF10A-Ctrl cells. *GAPDH* was used for normalization. Error bars are SEM of the fold change from three separate experiments, each in triplicate. $*P < 0.05$, $**P < 0.01$, $***P < 0.001$. (*D*) HCC1806ShNCT (2×10^5) cells were plated in a 6-cm Petri dish and transfected with 1.0 ng of full-length NCT cDNA (SC100655; Origene) and the pCMV6-XL4 empty vector control, using Lipofectamine 2000 (Invitrogen). Cells were incubated for 24 h and then lysed for mRNA and protein extraction. (*A*) RT-qPCR of *NCT, Vimenti*, and *Snail* showing a marked increase of relevant gene mRNA levels. $*P < 0.01$. *GAPDH* was used for normalizing. Error bars represent SD of two separate experiments.

cells were indeed a consequence of NCT depletion, we used a full-length NCT construct cloned into a pCMV6-XL4 expression vector, and transiently reconstituted NCT expression in HCC1806-ShNCT cells. This confirmed that reintroducing NCT in HCC1806-ShNCT cells was sufficient to induce transcription of the proinvasive genes *vimentin*, *SIP1*, *Snail1*, *MMP2*, and *MMP9* (Fig. S3*D*). Similar increase in the transcript levels of the proinvasive genes *SIP1*, *Snail1*, and *MMP2* was also observed upon transient transfection of the Notch1 ICD into HCC1806ShNCT cells, suggesting that NCT up-regulation may act through Notch1 to regulate proinvasive genes in breast cells (Fig. S3*E*).

Nicastrin Regulates EMT and Breast Cancer Stem Cells Through Notch and Akt Pathways. To assess the degree to which NCT-induced phenotypes in MCF10A cells were dependent on Notch and Akt signaling, we repressed GS by using a GSI (DAPT), and to specifically inhibit the activation of the Notch receptors whose cleavage was affected by NCT modulation, we used Notch1 siRNA (N1siRNA) and Notch4 siRNA (N4siRNA). We repressed PI3K/Akt signaling by using Wortmannin, LY294002 and a dominant negative AKT (DNAKT). We confirmed the effectiveness of the different treatments by assessing the levels of active Notch1/4 and pAkt, respectively (Fig. 4*A* and Fig. S4*A*). Notch1ICD levels in MCF10ANCT cells were attenuated by inhibition of Akt, whereas the up-regulation of Notch4ICD in MCF10ANCT compared with MCF10A-Ctrl cells persisted upon Akt inhibition (Fig. 4*A* and Fig. S4*A*). It appears that NCT induced regulation of Notch1 is achieved not only through GS but also through PI3K/Akt. Bidirectional cross-talk between Notch1 and Akt has been documented previously (30, 31).

Notch1/4 silencing and AKT inhibition partially revert the outgrowth of MCF10ANCT acini in 3D matrigel, because a heterogeneous population of both the small and the big acini remained upon these treatments (Fig. 4 *B* and *C* and Fig. S4*B*). The up-regulation of *Vimentin*, *MMP2*, *MMP9*, *Twist1*, *Snail1*, and *SIP1* in MCF10ANCT cells was restored to the levels of control cells upon Notch1/4 and/or Akt inhibition (Fig. 4*D* and Fig. S4*C*). Moreover, we found that DAPT and Notch1 inhibition rather than Notch4, were more potent in reducing NCT-induced expansion of $CD44^+/CD24^-$ and $ALDH^{high}$ BCSCs, and the formation of mammospheres (Fig. 4 *E* and *F* and Fig. S4 *D* and *E*), suggesting that NCT stimulates expansion of $CD44^+/CD24^-$ and $ALDH^{high}$ BCSCs mainly through the activation of Notch1.

Nicastrin Depletion Inhibits Tumor Formation in Vivo. To examine whether the effects of NCT depletion on BC cell growth and stem cell population would be maintained in vivo, we performed a s.c. serial dilution transplantation experiment in nude mice using HCC1806-ShLuc and HCC1806-ShNCT cells. Nicastrin depletion reduced tumor size as well as the success of engraftment in vivo (Fig. 5 *A*–*C*). The engraftment of tumors was progressively compromised as the number of HCC1806-ShNCT–injected cells was serially diluted, whereas the success of tumor uptake and growth was consistently maintained even upon serial dilution of HCC1806-ShLuc cells (Fig. 5 *C* and *D*). These results indicate that NCT expression is required for BCSC growth. NCT gene and protein expression were maintained at lower levels in HCC1806-ShNCT–derived tumors compared with those derived from HCC1806-ShLuc cells (Fig. 5 *E* and *F*). Consistent with our results in vitro, depletion of NCT reduced the expression levels of N1-ICD and pAkt in vivo (Fig. 5*E*). Notch target genes such as Hes1, Hey1, and Survivin were down-regulated. Importantly, Notch4 and Notch1 transcripts were significantly reduced in HCC1806-ShNCT tumors (Fig. 5*F*). Immunohistochemical analyses of the tumors revealed that the Ki67 proliferation index was comparable between HCC1806-ShLuc and ShNCT tumors (30–40%), despite a reduction in tumor size. By contrast, in the latter group, vimentin expression was strongly reduced (Fig. 5*G*). Taken together, these results suggest that NCT depletion compromises BC growth in vivo.

Finally, to assess whether NCT was able to transform MCF10A cells, we investigated the ability of MCF10ANCT cells to form colonies in soft agar and tumors when injected in the mammary fat pad of immunocompromised mice. Nicastrin overexpression in MCF10A cells was not sufficient to induce oncogenic transformation required for the colony or in vivo tumor formation. HCC1806-ShLuc and HCC1806-ShNCT cells were used as control, where we have observed successful colony formation in HCC1806-ShLuc cells, which was compromised in HCC1806-ShNCT cells, in line with our in vivo model (Fig. 5 and Fig. S5*A*).

Discussion

This work highlights the importance of NCT for expansion of $CD44^+/CD24^-$ and $ALDH1^{high}$ BCSC populations and their invasive features. We also show that NCT mediates this effect predominantly through Notch1, and importantly, demonstrate that depletion of NCT is sufficient to inhibit growth of a triple negative BC xenograft model in vivo. Our previous work has shown that NCT transient genetic silencing in MDAMB231 cells compromises their invasive capacity by affecting *vimentin*, *Snail*, and *Twist* (25).

Here, using shRNA oligos targeting *NCT* mRNA, distinct from those of the transient siRNA oligos (Fig. S5*B*), we analyzed the impact of stable NCT inhibition, and overexpression on breast cell morphology, invasive behavior, and maintenance of BCSCs. We used the triple negative BC cells, HCC1806, and a nontransformed breast cell line, MCF10A, respectively. As previously demonstrated (32–34), we show that NCT depletion in HCC1806 cells and stable

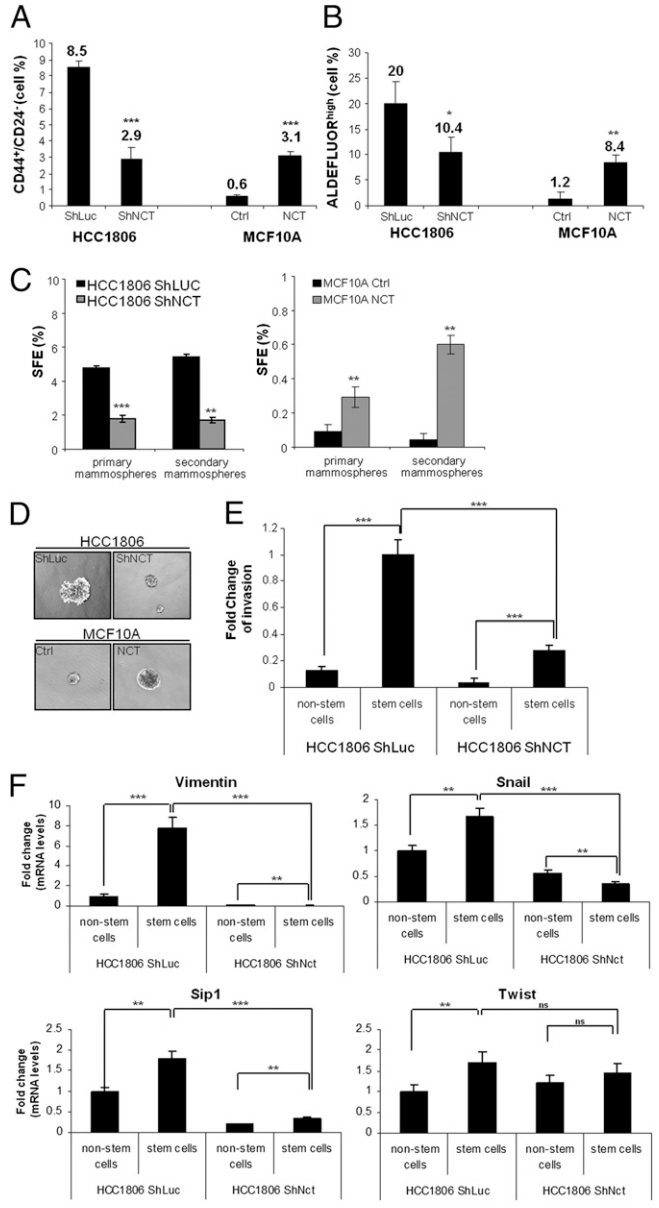

Fig. 3. Breast cancer stem cell population is affected by nicastrin expression. (*A*) Percentage of $CD44^+/CD24^-$ cells assessed by flow cytometry in HCC1806-ShLuc, HCC1806-ShNCT, MCF10A-Ctrl, and MCF10ANCT cell lines. Data are means ± SEM of three independent experiments. $***P < 0.001$. (*B*) Percentage of $ALDH^{high}$ cells assessed by flow cytometry in the same sample as in *A*. Data represent mean values ± SEM of three independent experiments. (*C*) Primary and secondary mammosphere forming efficacy of HCC1806-ShLuc, HCC1806-ShNCT, MCF10A-Ctrl, and MCF10ANCT cells. Sphere-forming efficacy (SFE) was calculated as the number of spheres formed in 10 d divided by the original number of single cells seeded and expressed as a percentage. Bars represent mean percentage of mammospheres ± SD from three separate experiments. (*D*) Representative images of mammospheres at day 10 of samples as in *C*. Magnification 20×. (*C*) Transwell invasion assay of nonstem ($CD44^+/CD24^-$-depleted cells) and stem cell ($CD44^+/CD24^-$ cells) FACS sorted populations from HCC1806-ShLuc and HCC1806-ShNCT cell lines. (*D*) Relative fold of *vimentin*, *Snail*, *Sip1*, and *Twist* gene expression levels in the same samples as in *C*. HCC1806-ShLuc nonstem cell population was used as calibrator. *GAPDH* was used for normalization. Data are expressed as mean ± SD of three independent experiments. $*P < 0.05$, $**P < 0.01$, $***P < 0.001$.

overexpression in MCF10A cells is able to disrupt and reconstitute, respectively, the expression of GS components PS1, Aph-1 and PEN-2, as well as GS activity, measured by Notch1- and Notch4 ICD. This result confirms the relevance of NCT in maintaining the stability and functionality of the GS complex in breast cells.

We have shown that in MCF10A and HCC1806 cells, respectively, NCT overexpression activates Notch1, Notch4, and Akt, whereas its depletion achieves the opposite effect. Others have shown that NCT modulates Akt activation in HEK293 cells (35). The impact we observe on the cellular Akt activation (pAkt Ser473), may be Notch1 mediated, because Notch1 activation can sustain Akt signaling in cancer cells (36, 37). Conversely, Notch1 siRNA or GSIs abrogate Akt activity (27). This is in line with our data, which show a reduction of elevated pAkt in MCF10ANCT cells upon treatment with the GSI and Notch1 siRNA.

Nicastrin overexpression in MCF10A cells induces proliferation only when cells grow in 3D Matrigel highlighting the importance of extracellular matrix (ECM) signaling in the context of NCT overexpression. Functional differences upon modulation of protein expression or use of inhibitors in cancer cells are often more readily

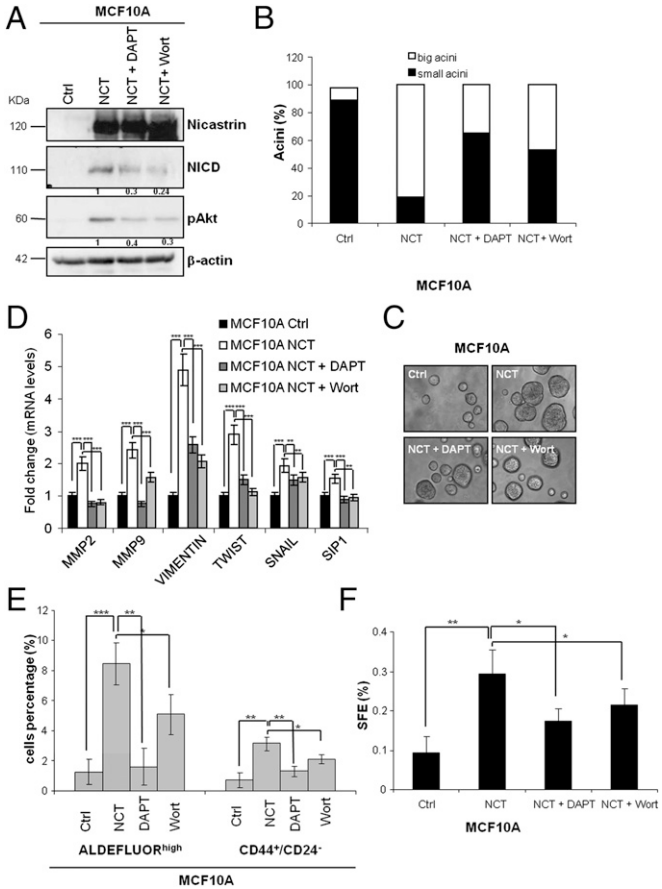

Fig. 4. Inhibition of Notch and AKT signaling pathways revert the malignant phenotype MCF0A-NCT in terms of EMT and stem cell content. (*A*) Immunoblot analysis of nicastrin, N1-ICD, and pAKT in MCF10ANCT cells, treated with DAPT or Wortamannin. Loading control was β-actin. (*B*) 3D assay of MCF10A-Ctrl, MCF10ANCT cells untreated, treated with DAPT, or Wortamannin. Bars are percentage of small and big acini structures observed after 10 d of culture. (*C*) Representative images of the different treatments are shown. Magnification 20×. (*D*) Relative fold of *MMP2*, *MMP9*, *Vimentin*, *Twist*, *Snail*, and *SIP1* gene expression levels in MCF10A-Ctrl, MCF10ANCT cells untreated, treated with DAPT, or Wortamannin for 3 d. *GAPDH* was used for normalization. Data are mean ± SD of three independent experiments. $*P < 0.05$, $**P < 0.01$, $***P < 0.001$. (*E*) Percentage of $CD44^+/CD24^-$ and $ALDH^{high}$ cells assessed by flow cytometry is sample as in *A*. Data are mean ± SD of three separate experiments. $*P < 0.05$, $**P < 0.01$, $***P < 0.001$. (*F*) Sphere forming efficacy of samples as in *A*. Data are means ± SD of three independent experiments. $*P < 0.05$, $**P < 0.01$.

CELL BIOLOGY

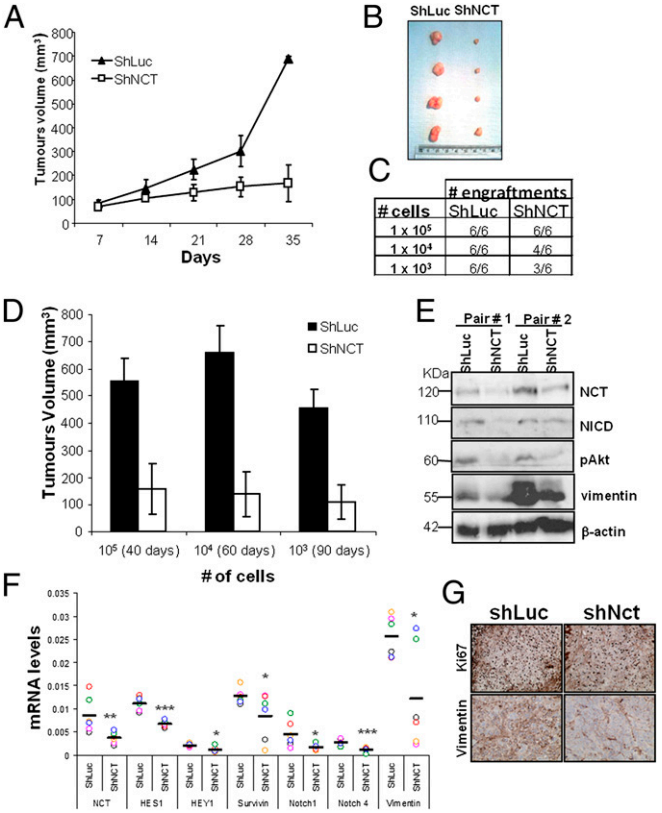

Fig. 5. Stable depletion of nicastrin in HCC1806 breast cancer cell line reduces tumor growth in vivo. (*A*) Size of s.c. tumor growth after injection of 1×10^6 HCC1806-ShLuc and HCC1806-ShNCT cells. Data are mean tumor size ± SD of six tumors per group. (*B*) Representative set of xenografts derived from injection of 10^6 HCC1806-ShLuc and HCC1806-ShNCT cells. (*C*) Table shows the number of tumor engraftments correlated with the number of HCC1806-ShLuc and HCC1806-ShNCT cells injected at serial dilution. (*D*) Tumor volumes of s.c. tumors obtained from the injection of 10^5, 10^4, and 10^3 HCC1806-ShLuc and HCC1806-ShNCT cells and collected at the indicated end points. (*E*) Representative immunoblot analysis of nicastrin, N1ICD, pAKT, and vimentin on HCC1806-ShLuc– and HCC1806-ShNCT–derived tumors. Each number (#) indicates tumor pairs obtained from the same mouse injected on the left flank with HCC1806-ShLuc cells and on the right flank with HCC1806-ShNCT cells. Loading control was assessed by β-actin. (*F*) Relative fold of *nicastrin*, *Hes1*, *Hey1*, *Survivin*, *Notch1*, and *Notch4* gene expression levels in HCC1806-ShLuc– and HCC1806-ShNCT–derived tumors. (*G*) Representative immunohistochemical analyses for H&E, Ki67, and vimentin on paraffin-embedded section of xenografts, generated by HCC1806-ShLuc and HCC1806-ShNCT cells.

observed in conditions such as 3D culture, which to a higher degree resembles the in vivo context (29, 38). Stimulation of acini growth in Matrigel cultures has already been observed upon Notch1 ICD overexpression in MCF10A cells (39). In MCF10ANCT cells treatment with DAPT, Wortmannin, LY294002, and DNAKT, partially reverted NCT-induced growth, suggesting that potentially other GS substrates (HER4, CD44, β1-integrin, etc.), could be responsible for the observed effects upon NCT overexpression.

Additionally, we found that NCT regulates proinvasive genes in breast cells. A panel of genes that drive EMT (vimentin, *SIP1*, *Snail1*, *Twist1*, *MMP2*, and *MMP9*) was unanimously inhibited in HCC1806-ShNCT cells, and up-regulated in MCF10ANCT cells. Regulation of vimentin was the most pronounced in both contexts and was coupled to a marked modulation of its transcriptional regulator *SIP1* (40). Simultaneous inhibition of all four Notch receptors by siRNA in other cell lines was capable of reducing vimentin protein levels (41). In our system, up-regulation of proinvasive genes upon NCT overexpression was reverted by DAPT, Notch1/4 siRNA, and Akt inhibition. Taken together with our data that place NCT in the Notch1/Akt signaling axis, it appears that NCT-induced effects on proinvasive genes are mediated mainly through Notch1. Accordingly, it has been reported that *Snail1* and *Twist1* are transcriptional targets of Notch1 (42, 43), and that both *MMP2* and *MMP9* can be modulated in various cell line models, including BC, by interfering with Notch1 (44–47). The molecular effects of NCT expression on proinvasive genes were further mirrored in the phenotypic change of HCC1806-ShNCT toward a more rounded cell shape, compact acini in 3D, and decreased invasiveness. Conversely, in MCF10A cells, NCT overexpression appears to switch on the EMT program to promoting breast cell invasiveness.

The relevance of the GS enzyme in human malignancies has been predominantly studied through Notch proteins (12). Recently, targeting NCT as the crucial structural and functional component of GS has emerged as a potential modality to disrupt the GS (25, 28, 48). Collectively, our data imply that NCT may have an important mechanistic role underlying the increased risk of dissemination of BC cells through regulation of vimentin, Snail1, and MMPs. Given the impact of NCT expression on the EMT signature of breast cells, and considering that cancer cells can acquire "stemness" features through EMT (6), we established that NCT expression affected not only the proportion of $CD44^+/CD24^-$ and $ALDH1^{high}$ BCSCs in HCC1806 and MCF10A cells, but also their ability to propagate in conditions sustaining the undifferentiated cell state, expression of proinvasive genes (*Vimentin*, *SIP1*, and *Twist1*), and invasive capacity. These effects of NCT appear to be mediated predominantly through Notch1 signaling, and partly through Notch4 and the Akt pathway, as determined by the reversal of NCT-induced effects upon silencing Notch1/4 and inhibiting Akt. The effect of NCT on the SFE is mediated through GS/Notch1 activity as DAPT and Notch1 siRNA reverted the potential of NCT-expressing stem cells to propagate in anchorage-independent conditions to baseline levels. This is in line with evidence that SFE in MCF-7, MDAMB231, BT474, and SKBR3 BC cells was abolished by using a GSI (MRK003).

When the effect of NCT overexpression on colony and tumor formation in MCF10A cells was evaluated, we recognized that overexpression of NCT alone fails to deliver a sufficiently potent oncogenic signal for bona fide malignant transformation. This is in line with the fact that overexpressed Notch1 and Notch4 collaborate with the Ras pathway to initiate tumors in vivo, whereas alone they also lack the ability to fully transform breast cells (49, 50).

However, we demonstrate that NCT inhibition in malignant breast cells can inhibit breast tumor formation in vivo. The fact that HCC1806-ShNCT tumors had delayed growth without a marked change in Ki67 tumor expression levels, and equally compromised success of tumor engraftment upon serial dilution implantation, signifies that the primary effect of NCT depletion may precisely be achieved by depleting BCSCs rather than differentiated tumor cells. Importantly, we also observed that Notch1 ICD protein and Notch1/4 mRNA, as well as proinvasive genes, were inhibited in tumors with reduced NCT expression.

Discovery of novel molecular targets to inhibit cancer metastases is of paramount importance (51). Considering that NCT depletion impedes BC cell growth and maintains low levels of Notch and proinvasive genes in vivo, reduces propagation, and invasion of BCSCs in vitro, we propose that anti-NCT therapy in BC may be relevant to reduce the number and the invasive potential of BCSCs, deemed responsible for cancer relapse.

Materials and Methods

Cell Lines/Treatments. HCC1806 ShLuc and HCC1806 ShNCT cells were cultured in the RPMI-1640 media (10% FCS and 2 mM L-glutamine, 100 units/mL penicillin, 0.1 mg/mL). A total of 2 μg/mL puromycin (Invitrogen) was added to media of infected cells. MCF10A were cultured in basal mammary epithelial cell growth medium with bovine pituitary extract (13 μg/mL), EGF (10 μg/mL), hydrocortisone (500 μg/mL), insulin (5 μg/mL), transferrin (0.005 μg/mL), cholera toxin (1 ng/mL), penicillin (100 units/mL), and streptomycin (0.1 mg/mL).

RNA Isolation, Quantitative RT-qPCR, and Western Blotting. These three techniques were performed as previously described (25). Primer sequences are provided in Table S1.

Sulforhodamine B (SRB) Colorimetric and Transwell Cell Invasion Assays. Sulforhodamine B colorimetric assay was used to assess cell proliferation. Transwell cell invasion assay was used to assess cell invasive capacity. Both were performed as previously described (52).

Mammosphere Culture. Mammosphere culture was used to assess capacity of BCSCs to propagate in anchorage-independent growth conditions.

In Vivo Tumorigenicity Assay. HCC1806-ShLuc and HCC1806-ShNCT cells were resuspended in the total volume of 100 μL containing 50% Matrigel were injected s.c. on the left and right flanks, respectively of 5- to 6-wk-old female BALB/c nude mice. Groups ($n = 6$) were injected with 10-fold serial dilutions (from 1×10^6 to 1×10^3 cells). Tumor growth rates were analyzed by caliper measurements once weekly. Tumor volume was calculated using the formula: (length × width)/2.

A detailed version of *Materials and Methods* is provided in *SI Materials and Methods*.

ACKNOWLEDGMENTS. We thank Prof. Gopal Thinakaran for providing us with the pMX-human nicastrin plasmid, and Cancer Research United Kingdom for supporting our work.

1. Zhou L, et al. (2010) The prognostic role of cancer stem cells in breast cancer: A meta-analysis of published literatures. *Breast Cancer Res Treat* 122:795–801.
2. Al-Hajj M, Wicha MS, Benito-Hernandez A, Morrison SJ, Clarke MF (2003) Prospective identification of tumorigenic breast cancer cells. *Proc Natl Acad Sci USA* 100:3983–3988.
3. Ginestier C, et al. (2007) ALDH1 is a marker of normal and malignant human mammary stem cells and a predictor of poor clinical outcome. *Cell Stem Cell* 1:555–567.
4. Kakarala M, Wicha MS (2007) Cancer stem cells: Implications for cancer treatment and prevention. *Cancer J* 13:271–275.
5. Takebe N, Harris PJ, Warren RQ, Ivy SP (2011) Targeting cancer stem cells by inhibiting Wnt, Notch, and Hedgehog pathways. *Nat Rev Clin Oncol* 8:97–106.
6. Mani SA, et al. (2008) The epithelial-mesenchymal transition generates cells with properties of stem cells. *Cell* 133:704–715.
7. Creighton CJ, Chang JC, Rosen JM (2010) Epithelial-mesenchymal transition (EMT) in tumor-initiating cells and its clinical implications in breast cancer. *J Mammary Gland Biol Neoplasia* 15:253–260.
8. Brabletz T, Jung A, Spaderna S, Hlubek F, Kirchner T (2005) Opinion: Migrating cancer stem cells: An integrated concept of malignant tumour progression. *Nat Rev Cancer* 5:744–749.
9. Jones RJ, Matsui WH, Smith BD (2004) Cancer stem cells: Are we missing the target? *J Natl Cancer Inst* 96:583–585.
10. De Strooper B (2003) Aph-1, Pen-2, and Nicastrin with Presenilin generate an active gamma-Secretase complex. *Neuron* 38:9–12.
11. De Strooper B, Annaert W (2010) Novel research horizons for presenilins and γ-secretases in cell biology and disease. *Annu Rev Cell Dev Biol* 26:235–260.
12. Rizzo P, et al. (2008) Rational targeting of Notch signaling in cancer. *Oncogene* 27:5124–5131.
13. Wang Z, et al. (2010) Targeting Notch signaling pathway to overcome drug resistance for cancer therapy. *Biochim Biophys Acta* 1806:258–267.
14. Sharma A, Paranjape AN, Rangarajan A, Dighe RR (2012) A monoclonal antibody against human Notch1 ligand binding domain depletes subpopulation of breast cancer stem-like cells. *Mol Cancer Ther* 11:77–86.
15. Kondratyev M, et al. (2012) Gamma-secretase inhibitors target tumor-initiating cells in a mouse model of ERBB2 breast cancer. *Oncogene* 31:93–103.
16. McGowan PM, et al. (2011) Notch1 inhibition alters the CD44hi/CD24lo population and reduces the formation of brain metastases from breast cancer. *Mol Cancer Res* 9:834–844.
17. Harrison H, et al. (2010) Regulation of breast cancer stem cell activity by signaling through the Notch4 receptor. *Cancer Res* 70:709–718.
18. Farnie G, Clarke RB (2007) Mammary stem cells and breast cancer—role of Notch signalling. *Stem Cell Rev* 3:169–175.
19. Wei P, et al. (2010) Evaluation of selective gamma-secretase inhibitor PF-03084014 for its antitumor efficacy and gastrointestinal safety to guide optimal clinical trial design. *Mol Cancer Ther* 9:1618–1628.
20. van Es JH, et al. (2005) Notch/gamma-secretase inhibition turns proliferative cells in intestinal crypts and adenomas into goblet cells. *Nature* 435:959–963.
21. Tolcher AW, et al. (2010) A phase I study of RO4929097, a novel gamma secretase inhibitor, in patients with advanced solid tumors. 2006 American Society of Clinical Oncology Annual Meeting Proceedings, Part I, Vol 28. Available at http://www.asco.org/ASCOv2/Meetings/Abstracts?&vmview=abst_detail_view&confID=74&abstractID=43434. Accessed September 13, 2012.
22. Robinson DR, et al. (2011) Functionally recurrent rearrangements of the MAST kinase and Notch gene families in breast cancer. *Nat Med* 17:1646–1651.
23. Arcaroli J, Dasari A, Wessersmith WA, Jimeno A (2011) Gamma-secretase inhibitors in solid tumor malignancies. *Drugs Future* 36:677–689.
24. De Strooper B (2005) Nicastrin: Gatekeeper of the gamma-secretase complex. *Cell* 122:318–320.
25. Filipović A, et al. (2011) Biological and clinical implications of nicastrin expression in invasive breast cancer. *Breast Cancer Res Treat* 125:43–53.
26. Dong Y, Li A, Wang J, Weber JD, Michel LS (2010) Synthetic lethality through combined Notch-epidermal growth factor receptor pathway inhibition in basal-like breast cancer. *Cancer Res* 70:5465–5474.
27. Meng RD, et al. (2009) gamma-Secretase inhibitors abrogate oxaliplatin-induced activation of the Notch-1 signaling pathway in colon cancer cells resulting in enhanced chemosensitivity. *Cancer Res* 69:573–582.
28. Hayashi I, et al. (2012) Neutralization of the gamma-secretase activity by monoclonal antibody against extracellular domain of nicastrin. *Oncogene* 31:787–798.
29. Kenny PA, et al. (2007) The morphologies of breast cancer cell lines in three-dimensional assays correlate with their profiles of gene expression. *Mol Oncol* 1:84–96.
30. McKenzie G, et al. (2006) Cellular Notch responsiveness is defined by phosphoinositide 3-kinase-dependent signals. *BMC Cell Biol* 7:10.
31. Meurette O, et al. (2009) Notch activation induces Akt signaling via an autocrine loop to prevent apoptosis in breast epithelial cells. *Cancer Res* 69:5015–5022.
32. Zhang YW, et al. (2005) Nicastrin is critical for stability and trafficking but not association of other presenilin/gamma-secretase components. *J Biol Chem* 280:17020–17026.
33. Shirotani K, et al. (2003) Gamma-secretase activity is associated with a conformational change of nicastrin. *J Biol Chem* 278:16474–16477.
34. Shirotani K, Edbauer D, Kostka M, Steiner H, Haass C (2004) Immature nicastrin stabilizes APH-1 independent of PEN-2 and presenilin: identification of nicastrin mutants that selectively interact with APH-1. *J Neurochem* 89:1520–1527.
35. Pardossi-Piquard R, et al. (2009) p53-dependent control of cell death by nicastrin: Lack of requirement for presenilin-dependent gamma-secretase complex. *J Neurochem* 109:225–237.
36. Yao J, Qian C (2010) Inhibition of Notch3 enhances sensitivity to gemcitabine in pancreatic cancer through an inactivation of PI3K/Akt-dependent pathway. *Med Oncol* 27:1017–1022.
37. Gutierrez A, Look AT (2007) NOTCH and PI3K-AKT pathways intertwined. *Cancer Cell* 12:411–413.
38. Pickl M, Ries CH (2009) Comparison of 3D and 2D tumor models reveals enhanced HER2 activation in 3D associated with an increased response to trastuzumab. *Oncogene* 28:461–468.
39. Mazzone M, et al. (2010) Dose-dependent induction of distinct phenotypic responses to Notch pathway activation in mammary epithelial cells. *Proc Natl Acad Sci USA* 107:5012–5017.
40. Bindels S, et al. (2006) Regulation of vimentin by SIP1 in human epithelial breast tumor cells. *Oncogene* 25:4975–4985.
41. Dang H, et al. (2009) Role for Notch signaling in salivary acinar cell growth and differentiation. *Dev Dyn* 238:724–731.
42. Chen J, Imanaka N, Chen J, Griffin JD (2010) Hypoxia potentiates Notch signaling in breast cancer leading to decreased E-cadherin expression and increased cell migration and invasion. *Br J Cancer* 102:351–360.
43. Leong KG, et al. (2007) Jagged1-mediated Notch activation induces epithelial-to-mesenchymal transition through Slug-induced repression of E-cadherin. *J Exp Med* 204:2935–2948.
44. Funahashi Y, et al. (2011) Notch modulates VEGF action in endothelial cells by inducing matrix metalloprotease activity. *Vasc Cell* 3:2.
45. Bin Hafeez B, et al. (2009) Targeted knockdown of Notch1 inhibits invasion of human prostate cancer cells concomitant with inhibition of matrix metalloproteinase-9 and urokinase plasminogen activator. *Clin Cancer Res* 15:452–459.
46. Wang J, Fu L, Gu F, Ma Y (2011) Notch1 is involved in migration and invasion of human breast cancer cells. *Oncol Rep* 26:1295–1303.
47. Wang Z, et al. (2006) Down-regulation of notch-1 inhibits invasion by inactivation of nuclear factor-kappaB, vascular endothelial growth factor, and matrix metalloproteinase-9 in pancreatic cancer cells. *Cancer Res* 66:2778–2784.
48. Hayashi I, et al. (2009) Single chain variable fragment against nicastrin inhibits the gamma-secretase activity. *J Biol Chem* 284:27838–27847.
49. Mittal S, Subramanyam D, Dey D, Kumar RV, Rangarajan A (2009) Cooperation of Notch and Ras/MAPK signaling pathways in human breast carcinogenesis. *Mol Cancer* 8:128.
50. Fitzgerald K, Harrington A, Leder P (2000) Ras pathway signals are required for notch-mediated oncogenesis. *Oncogene* 19:4191–4198.
51. Giamas G, et al. (2011) Kinome screening for regulators of the estrogen receptor identifies LMTK3 as a new therapeutic target in breast cancer. *Nat Med* 17:715–719.
52. Rasul S, et al. (2009) Inhibition of gamma-secretase induces G2/M arrest and triggers apoptosis in breast cancer cells. *Br J Cancer* 100:1879–1888.